Science Advances
AAAS

Supplementary Materials for

Circadian disruption enhances HSF1 signaling and tumorigenesis in *Kras*-driven lung cancer

Marie Pariollaud *et al.*

Corresponding author: Katja A. Lamia, klamia@scripps.edu

Sci. Adv. **8**, eabo1123 (2022)
DOI: 10.1126/sciadv.abo1123

This PDF file includes:

Figs. S1 to S13

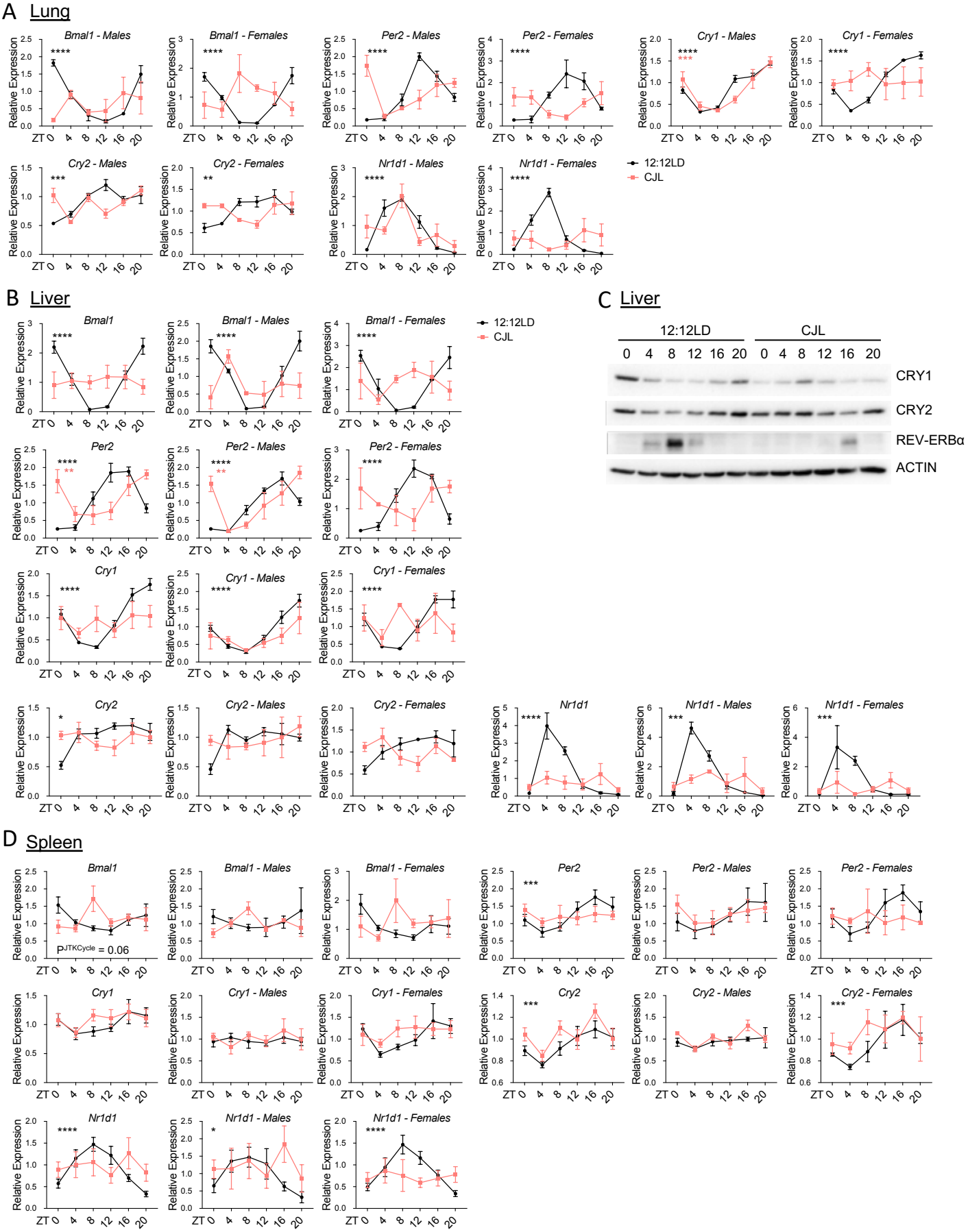

Fig. S1. Core clock gene expression in multiple tissues from mice housed in 12:12LD or chronic jetlag (CJL) conditions. C57BL/6J male and female mice were housed in 12:12LD or CJL for 8 weeks. Tissues were collected at the indicated times (hours after lights on) on Day 1 of the schedule shown in Fig. 1A. **(A,B,D)** Gene expression normalized to *U36b4* measured by quantitative real-time PCR from lungs (A), livers (B) and spleen (D). Data represent mean ± SEM for 3 males and 3 females per time point and light condition, both sexes plotted together or separately. Rhythmicity was determined by JTK_Cycle analyses; *$P^{JTKCycle}$ <0.05, **$P^{JTKCycle}$ <0.01, ***$P^{JTKCycle}$ <0.001 and ****$P^{JTKCycle}$ <0.0001. (C) Proteins detected by immunoblot from livers. Each lane on the Western blot represents a sample prepared from a unique animal. Representative images were taken from n = 6 biological replicates.

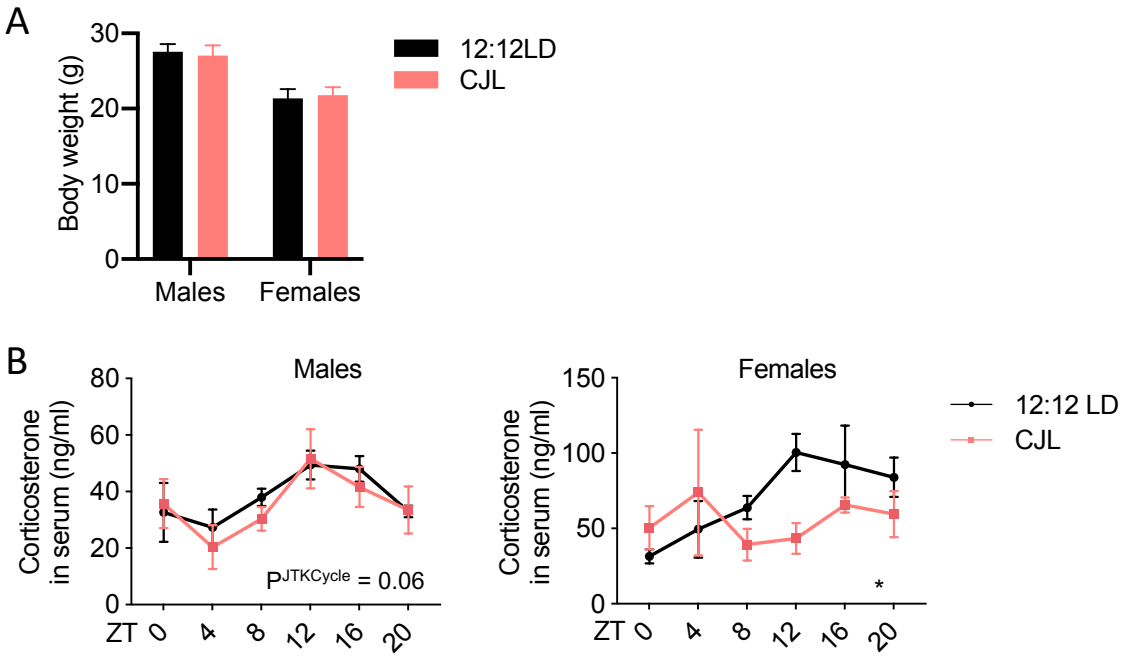

Fig. S2. Body weight and serum corticosterone levels from mice housed in 12:12LD or chronic jetlag (CJL) conditions. C57BL/6J male and female mice were housed in 12:12LD or CJL for 8 weeks. **(A)** Weights were recorded prior to euthanasia. **(B)** Corticosterone levels in serum were measured from blood samples collected at the indicated times (hours after lights on) on Day 1 of the schedule shown in Fig. 1A. Data represent mean ± SEM for 3 males and 3 females per time point and light condition. Rhythmicity was determined by JTK_Cycle analyses; *$P^{JTKCycle}$ <0.05.

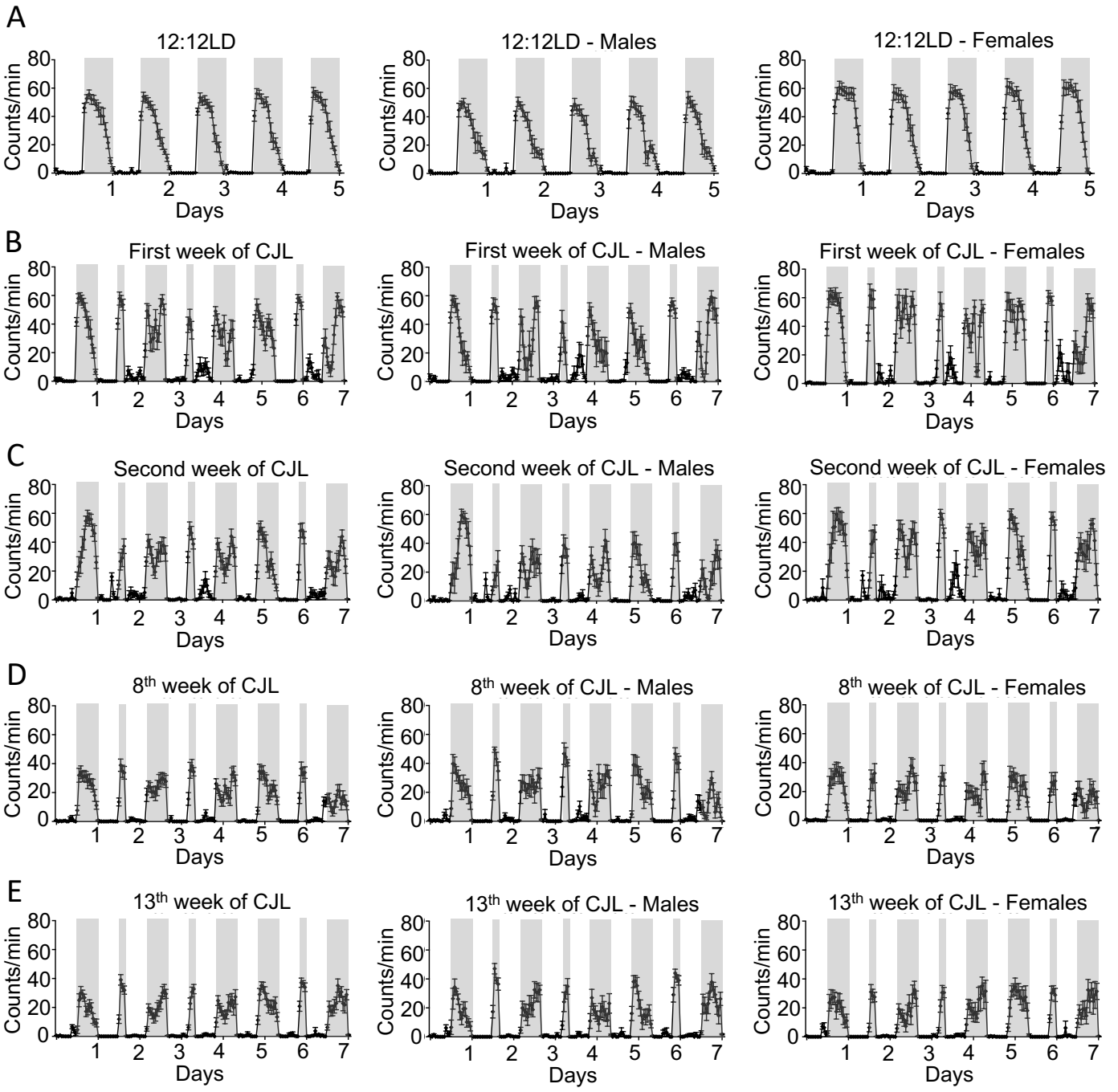

Fig. S3. Wheel-running activity. (A-E) 8-weeks old C57BL/6J male and female mice were housed in 12:12LD for 2 weeks and then in CJL for 13 weeks in presence of a running wheel. Group mean waveforms of wheel running activity for the last 5 days in 12:12LD (A), first (B), second (C), eighth (D) and thirteenth (E) week in CJL conditions. Data represent mean ± SEM for 8 males and 8 females, plotted together or separately. Grey rectangles represent dark phases.

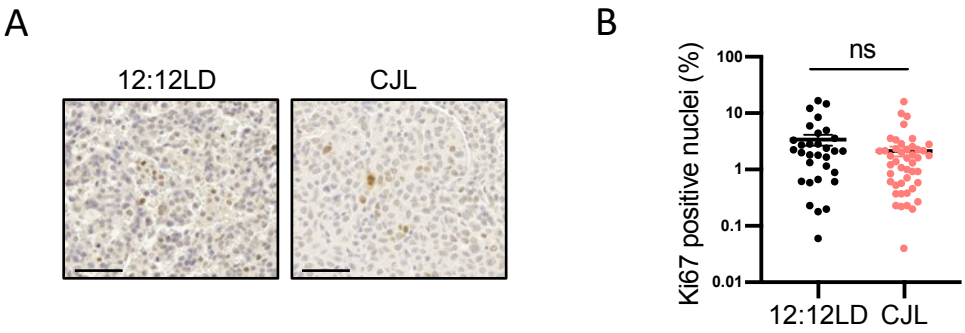

Fig. S4. Ki67 protein levels in tumors from K mice exposed to CJL or normal light conditions. Five weeks post-infection with lentivirus-Cre, K mice were placed in either 12:12LD or CJL for 20 weeks. **(A)** Representative Ki67 IHC images in tumors from K mice sacrificed at ZT5; scale bar, 50 μm. **(B)** Quantitation of stained positive nuclei.

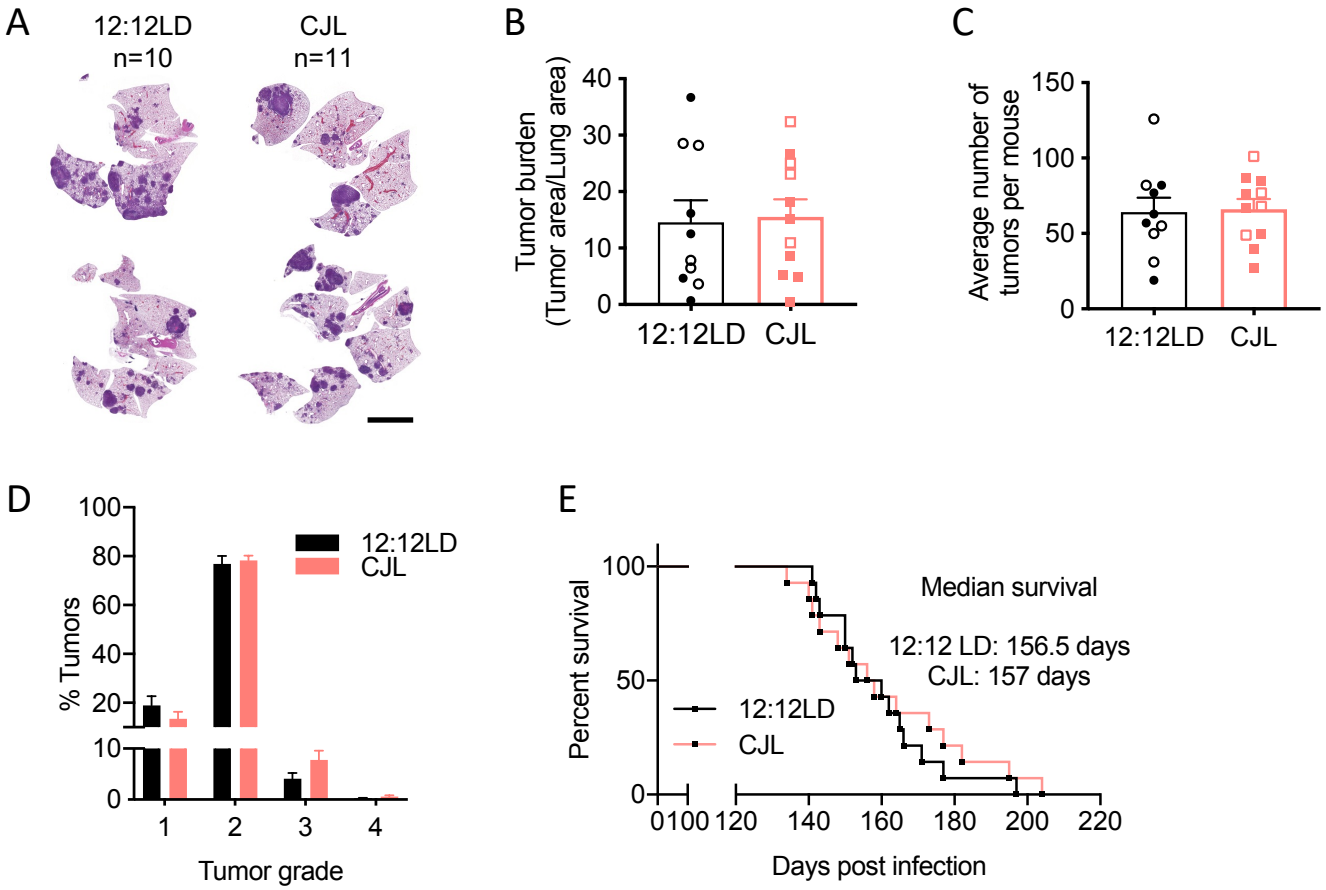

Fig. S5. Tumor burden and overall survival in KP mice exposed to 12:12LD or CJL. Five weeks post-infection with lentivirus-Cre, KP mice were placed in either 12:12LD or CJL for 10 weeks (A-D) or until signs of distress (E). **(A)** Representative H&E-stained sections at endpoint; scale bar, 5000 μm. Tumor burden **(B)**, numbers **(C)**, and grade **(D)** were assessed from H&E sections. Column data represent mean ± SEM. Values for individual animals are plotted, clear and filled symbols represent males and females respectively. **(E)** Kaplan-Meier survival analysis for K mice placed in 12:12LD (n = 14) or CJL (n = 14) conditions.

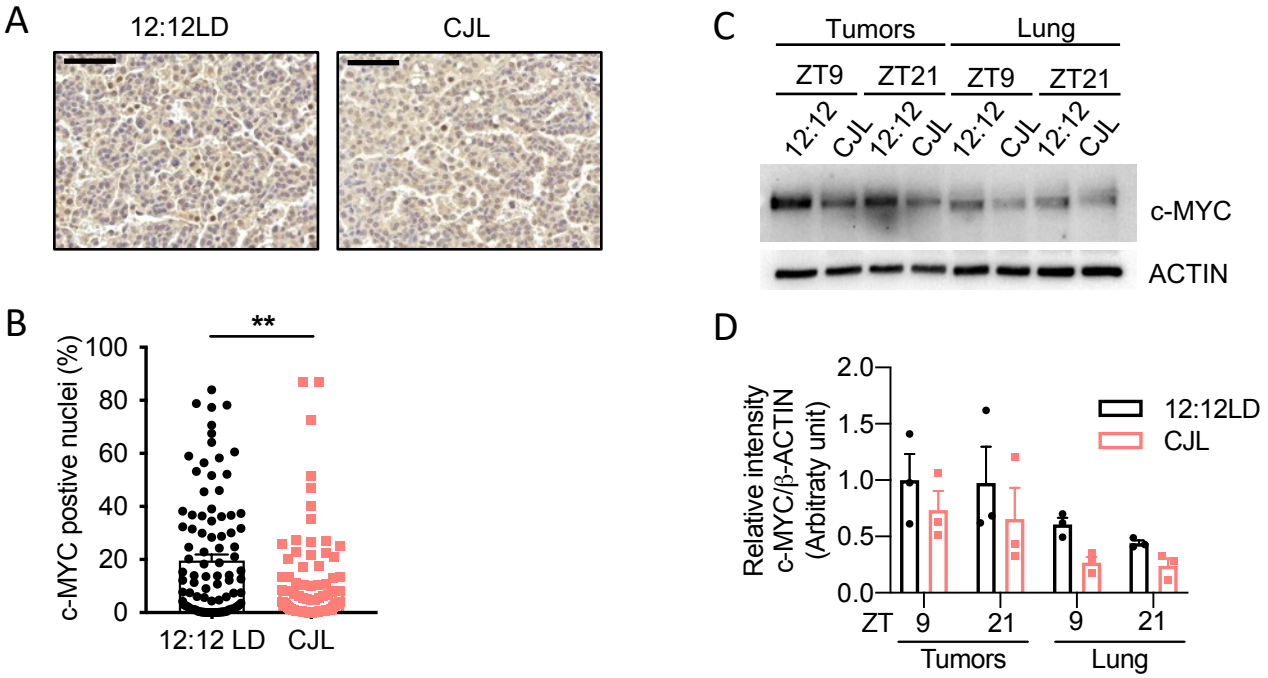

Fig. S6. c-MYC protein levels in tumors and lungs from K mice exposed to CJL or normal light conditions. Five weeks post-infection with lentivirus-Cre, K mice were placed in either 12:12LD or CJL for 20 weeks. **(A)** Representative c-MYC IHC images in tumors from K mice sacrificed at ZT5; scale bar, 50 μm. **(B)** Quantitation of stained positive nuclei. **P <0.01 by Mann-Whitney test. **(C)** c-MYC detected by immunoblot. Tumors and lungs for each light condition and time point on the blot were from the same animal. Representative images were taken from n = 3 biological replicates. **(D)** Quantitation of (C).

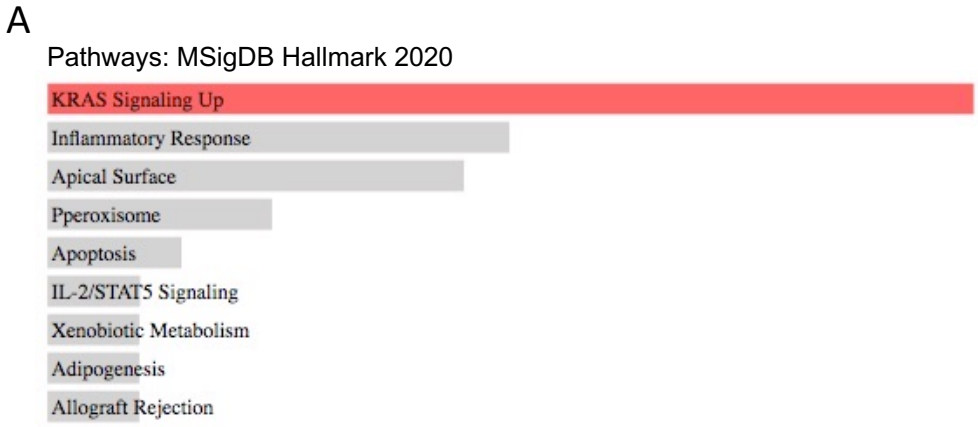

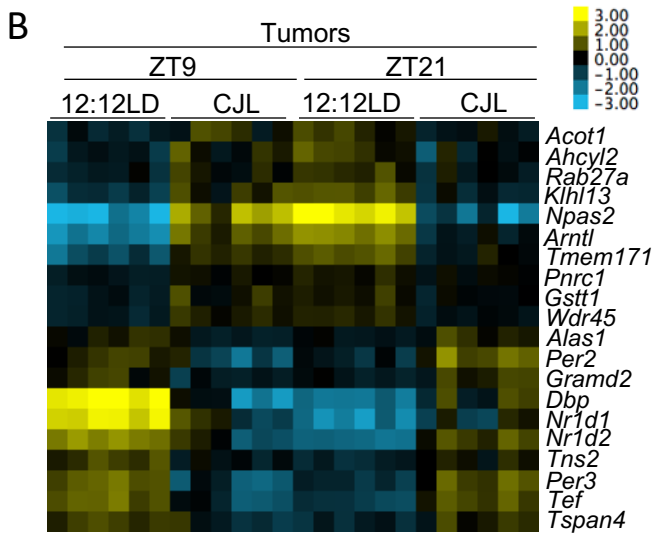

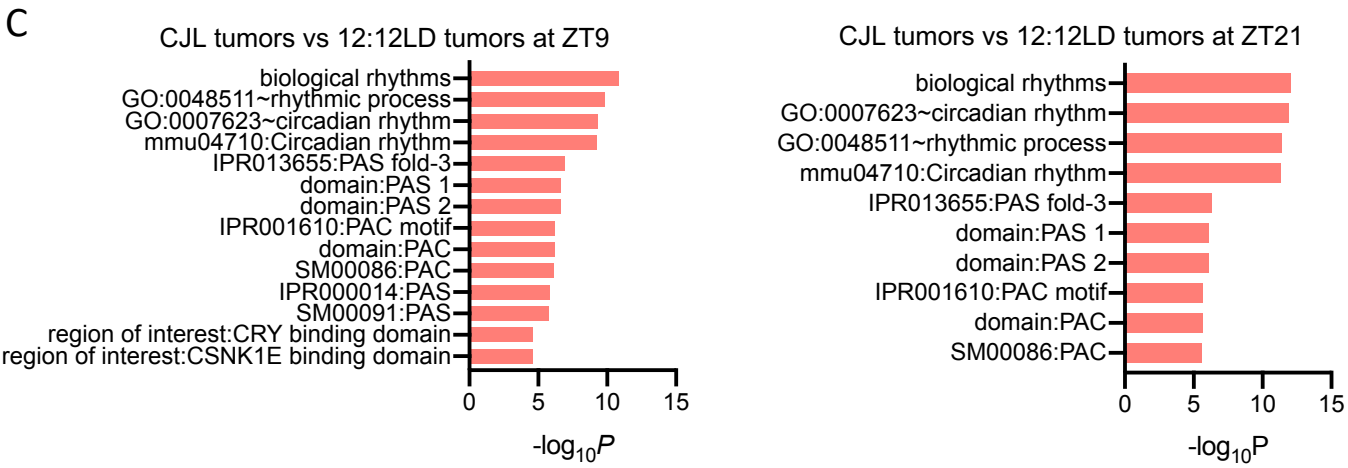

Fig. S7. RNA-seq data analyses on lungs and tumors collected from K mice exposed to 12:12LD or CJL. Five weeks post-infection with lentivirus-Cre, K mice were placed in either 12:12LD or CJL for 20 weeks. (A) Enrichr Pathway analysis of the upregulated genes in tumors compared to whole lungs (48 genes with log2FoldChange >= 1.5), all conditions combined, sorted by p-value ranking. Colored bar correspond to terms with significant p-values (<0.05). (B) Heatmap of the 20 genes differentially expressed upon CJL versus 12:12LD in tumors at both ZT9 and ZT20. **(C)** DAVID analyses on the differentially expressed genes in tumors between 12:12LD and CJL. Only terms with FDR< 0.25 are shown.

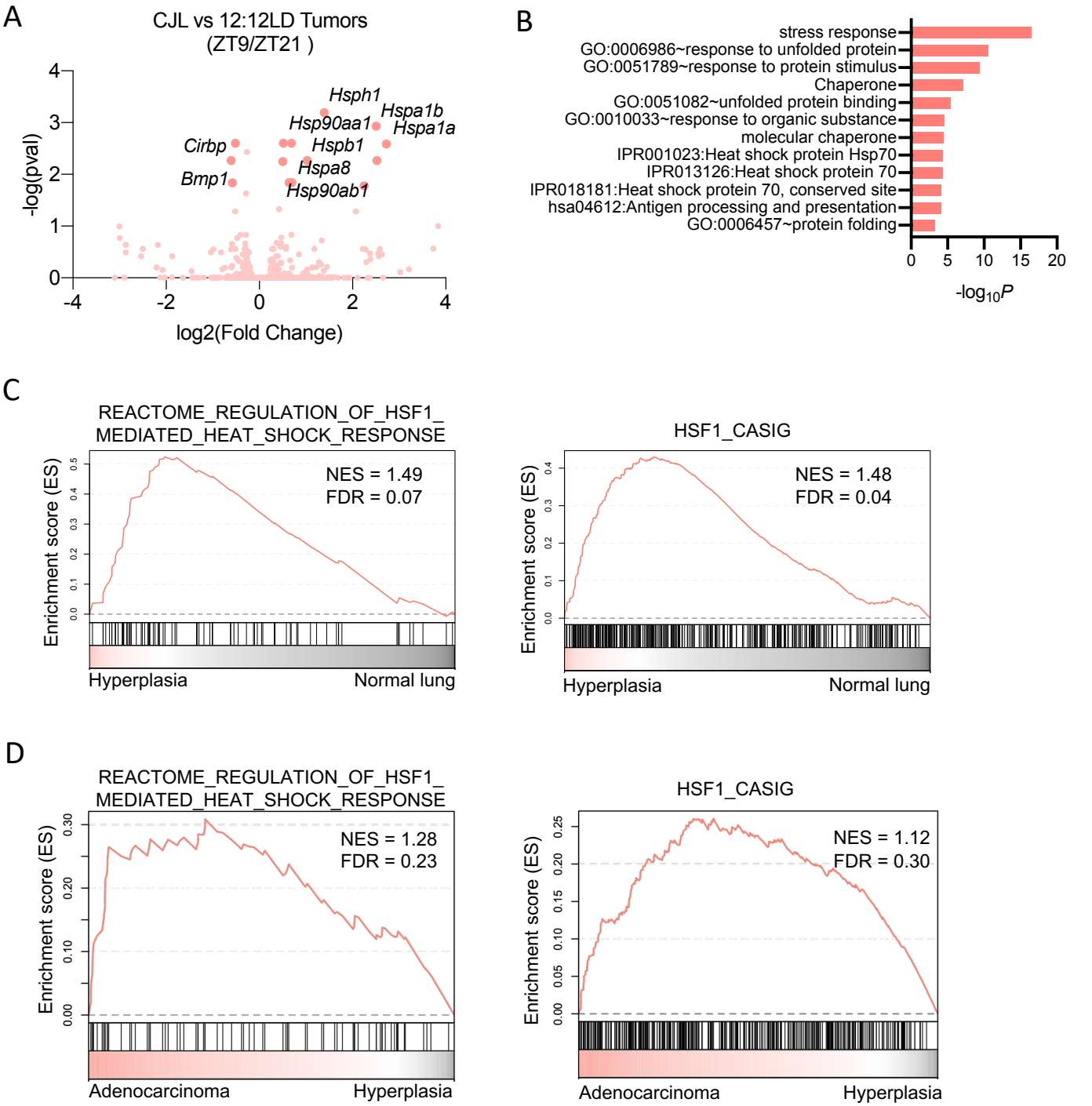

Fig. S8. Up-regulation of HSF1-mediated heat shock response and cancer signature in mouse models of Kras-driven lung cancer. (A,B) Five weeks post-infection with lentivirus-Cre, K mice were placed in either 12:12LD or CJL for 20 weeks. **(A)** Volcano plots of differentially expressed genes between 12:12LD and CJL by DESeq2 analyses for tumors only, taking time of collection (ZT9/21) as confounding factor. **(B)** DAVID analyses on the differentially expressed genes by DESeq2 in tumors between 12:12LD and CJL, taking time of collection as confounding factor. Only terms with FDR< 0.25 are shown. **(C-D)** GSEA plots for the HSF1-mediated heat shock response reactome and HSF1-Cancer signature gene sets applied to microarray data of laser-capture microdissected hyperplasic or normal lung cells (*52*) (C) and adenocarcinoma or hyperplasic lesions (D) from K-Ras^{G12V} mice.

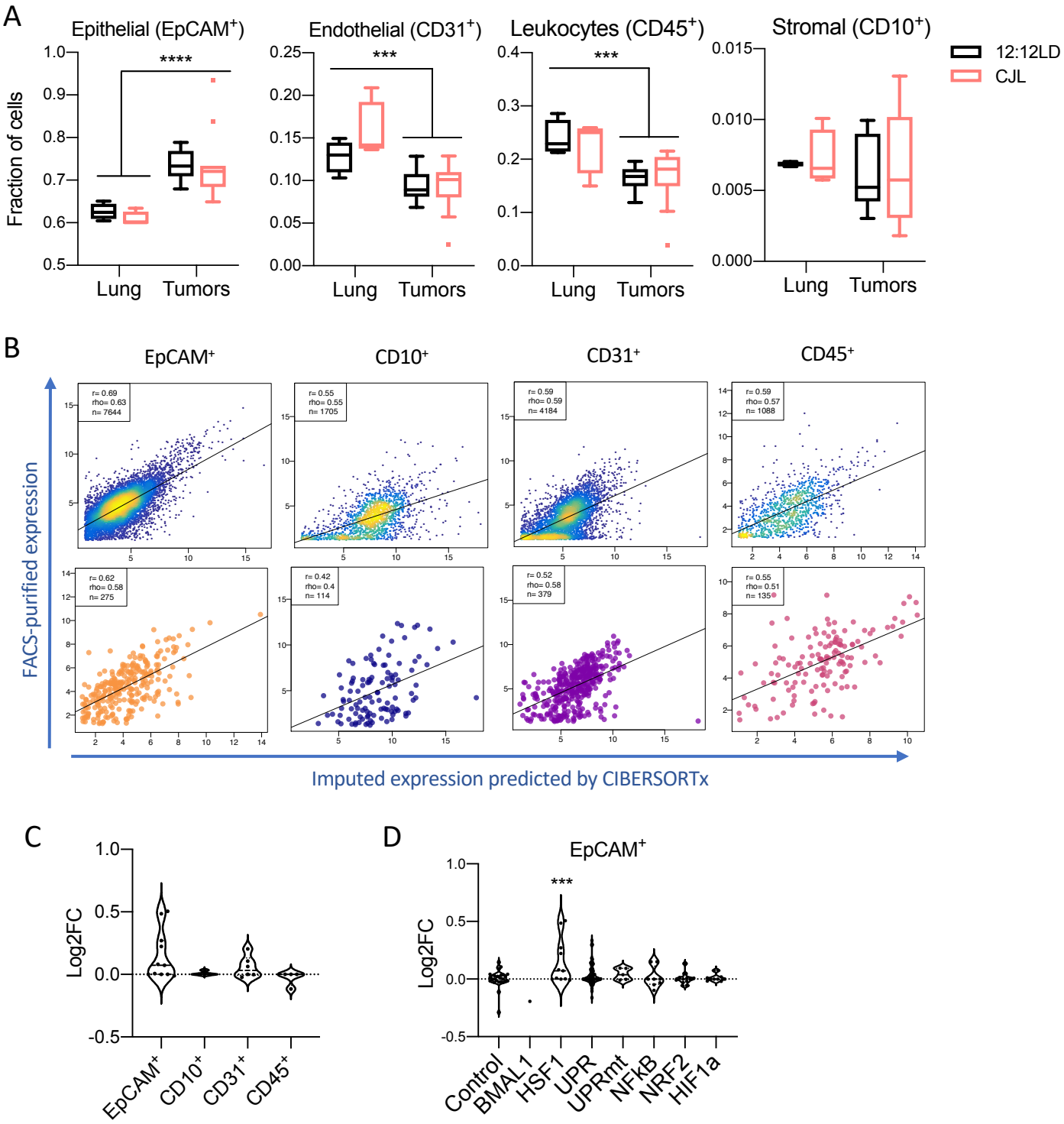

Fig. S9. Cell fractions and imputed expression in tumors and whole lung samples from K mice. (A) Imputed cell fractions from deconvolution of our RNA-sequencing data using CIBERSORTx and sigmatrix_NSCLC. **(B)** Scatter plots comparing expression profiles of mathematically purified (x axis) and observed expression values in a control "groundtruth" dataset (top) or in the signature matrix (sigmatrix_NSCLC; bottom) from RNA sequencing performed in FACS-sorted samples from human non small cell lung cancer biopsies. **(C)** Visualization of mean group fold changes of imputed expression of genes established as selective targets of HSF1 stress pathway (*49*) in each cell type. **(D)** Visualization of mean group fold changes of imputed expression of genes established as selective targets of each stress pathways (*49*) or "BMAL1-pathway" (*43*) in EpCAM+ cells. *** P < 0.001 by one-Way ANOVA with Dunnett's multiple comparison test. Note: Transcripts (including *Hspa1a, Hspa1b,* and several BMAL1 targets) for which expression could not be reliably imputed are omitted.

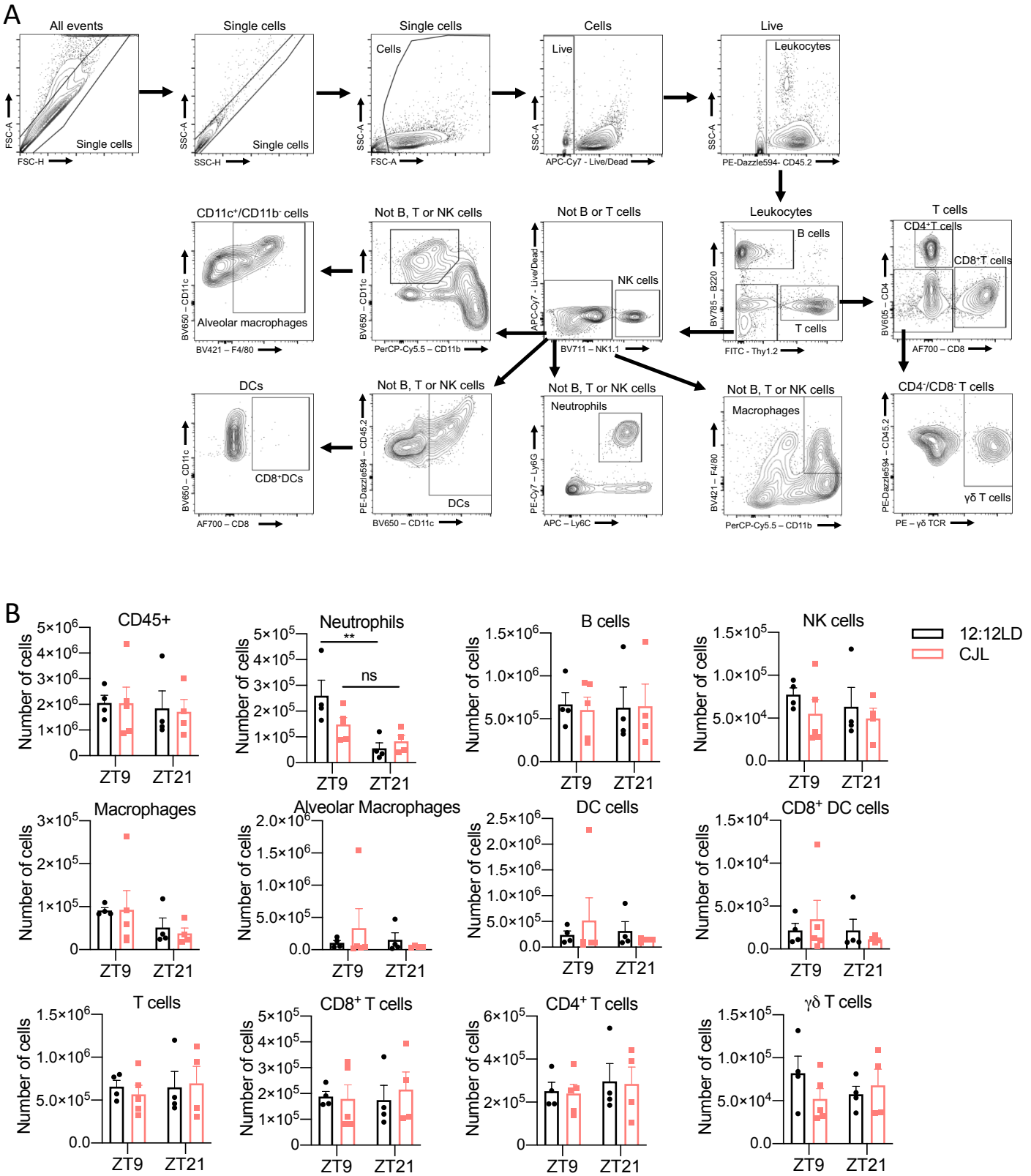

Fig. S10. Flow cytometry gating strategy and immune cell numbers. Five weeks post-infection with lentivirus-Cre, K mice were placed in either 12:12LD or CJL for 20 weeks. **(A)** Flow cytometry gating strategy. **(B)** Immune cell counts. *n*=4 for each time time point and lightning condition. **P <0.01 by two-Way ANOVA, post hoc Bonferroni test.

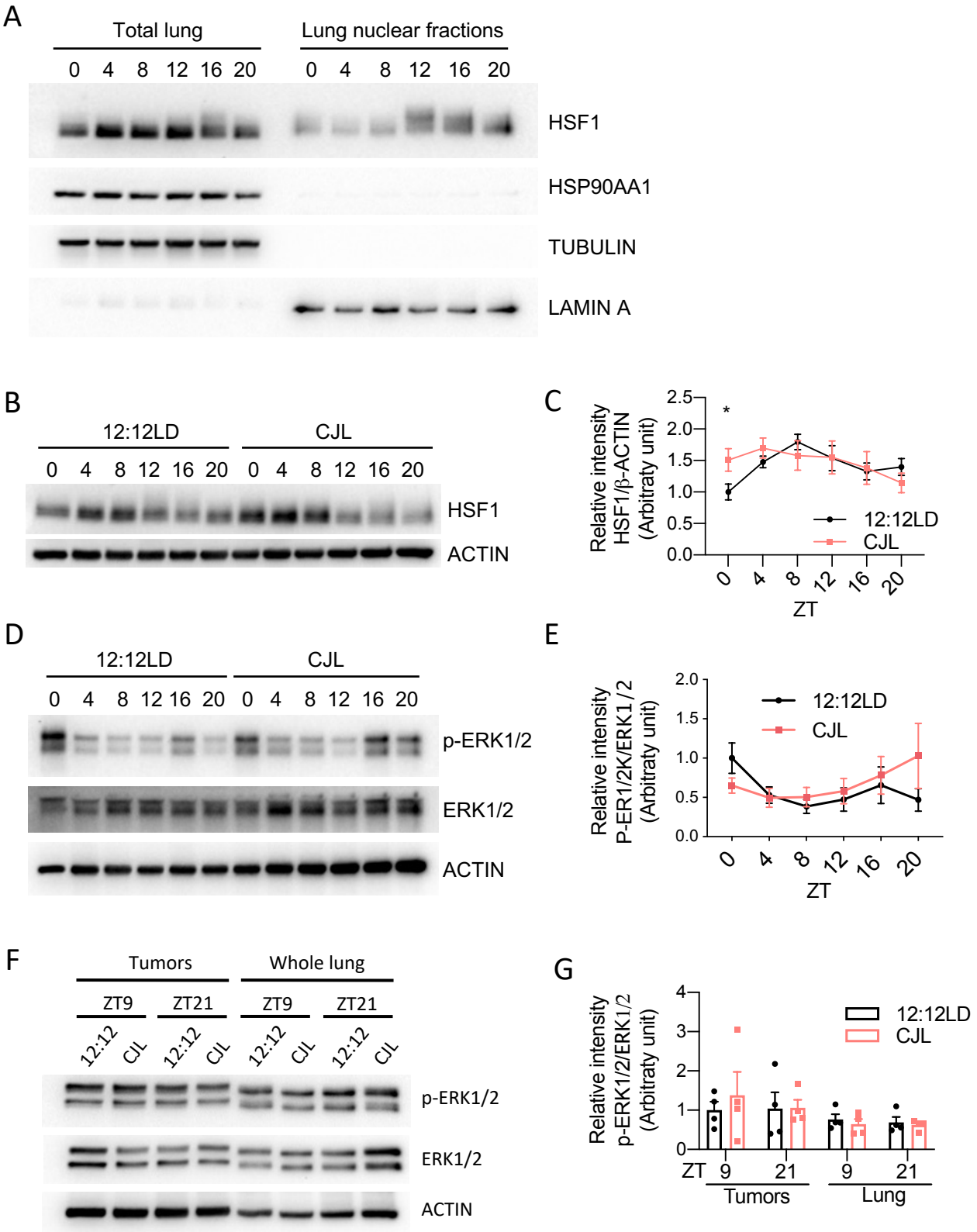

Fig. S11. HSF1 protein levels in lung. (A) Proteins from whole lung or lung nuclear extracts detected by immunoblot from C57BL/6J mice housed in 12:12LD for 8 weeks. Lung tissues were collected at the indicated times (hours after lights on). Each lane on the Western blot represents a sample prepared from a unique animal. **(B,D)** Proteins from whole lungs detected by immunoblot from the same cohort of C57BL/6J as in Fig. 1. Each lane on the Western blot represents a sample prepared from a unique animal. Representative images were taken from *n* = 3 biological replicates. **(C,E)** Quantitation of (B) and (D) respectively. Rhythmicity was determined by JTK_Cycle analyses; *$P^{JTKCycle}$ <0.05. **(F)** Proteins detected by immunoblot from tumors and lung tissue from K mice housed in 12:12LD or CJL for 20 weeks. Tumors and lungs for each light condition and time point on the blot were from the same animal. Representative images were taken from n = 4 biological replicates. (G) Quantitation of (F).

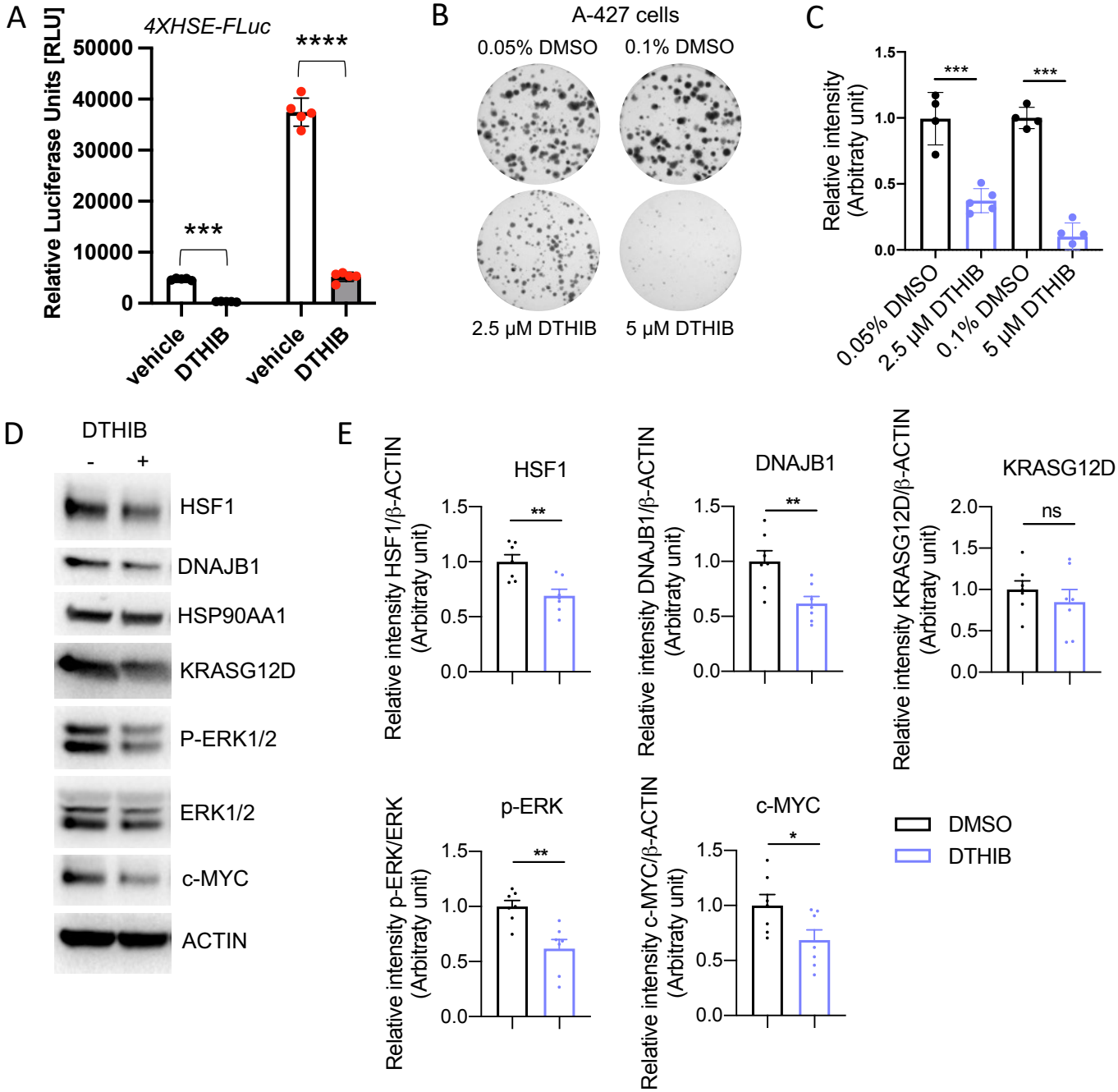

Fig. S12. Pharmacological inhibition of HSF1 using DTHIB. (A) Relative luciferase activity in HEK293T cells stably expressing the reporter *pGL4.41Luc2P/4XHSE/Hygro* and treated with vehicle (black symbols) or the HSF1 activator A3 (red symbols) and vehicle (open bars) or 5 μM DTHIB (filled gray bars). *** P < 0.001, **** P < 0.0001 by two-way ANOVA. **(B)** Representative images of crystal violet stained colonies formed by A-427 cells treated with DTHIB or vehicle DMSO 7 days after seeding, for 9 days. **(C)** Quantification of (B) from three biological replicates. Each condition was compared to controls that were plated in wells on the same plates. Bars represent mean ± SD, **P < 0.01 by student t-test. **(D)** Immunoblot of A-427 cells treated with 5 μM DTHIB or 0.1% DMSO for 48h. Representative of n=7. **(E)** Quantitation of (D).

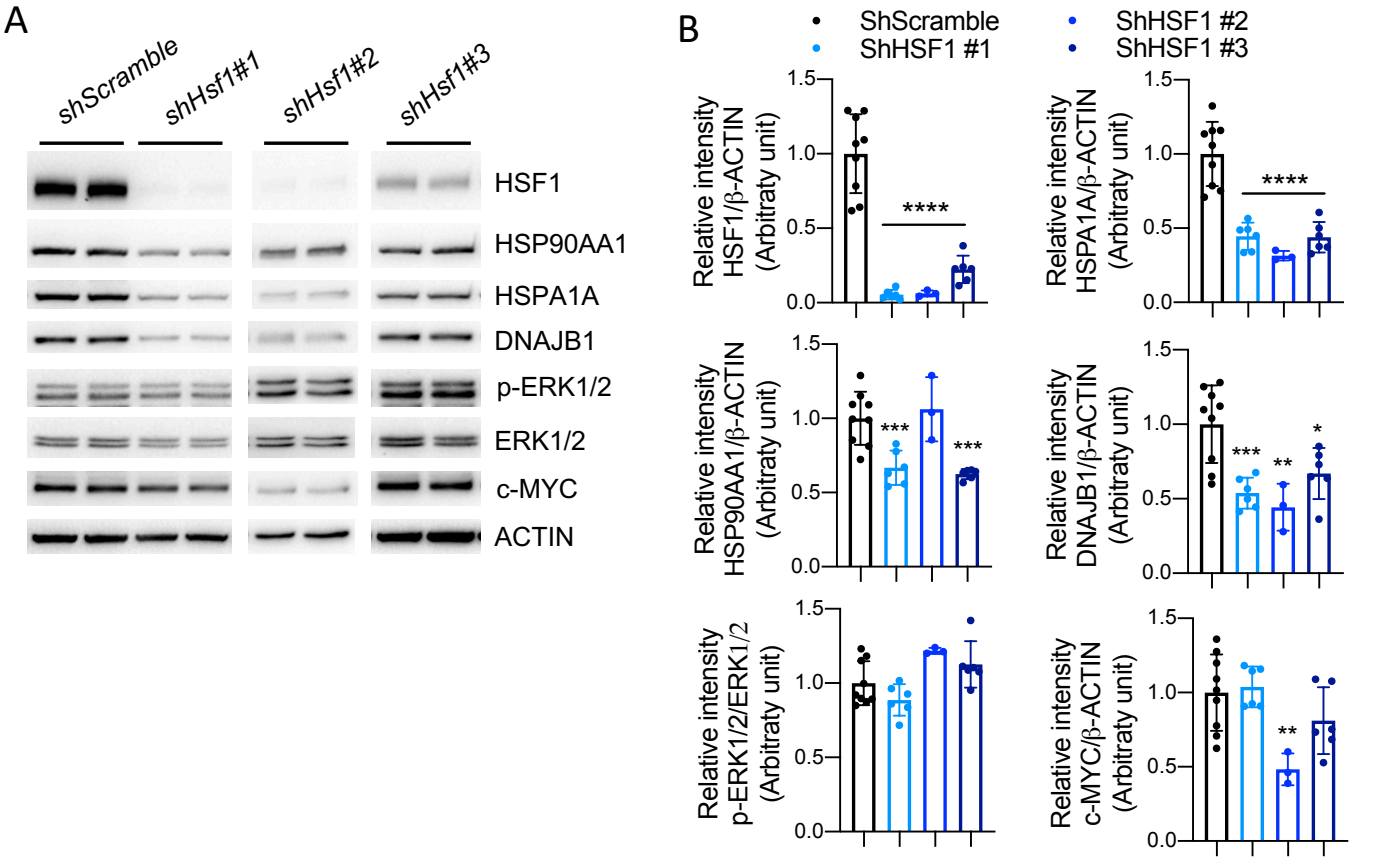

Fig. S13. Genetic inhibition of HSF1 by shRNAs. (A) Immunoblot of A-427 cells subjected to shRNAs targeting *HSF1*. Representative of n=3-6. **(B)** Quantitation of (A); bars represent mean ± SD, *P < 0.05, **P < 0.01, ***P < 0.001, ****P < 0.0001 relative to ShScramble by one-way ANOVA, post hoc Bonferroni test.